NITRIC OXIDE: Biology and Chemistry
Vol. 6, No. 1, pp. 18–28 (2002)
doi:10.1006/niox.2001.0383, available online at http://www.idealibrary.com on IDEAL®

Endotoxin-Induced Liver Hypoxia: Defective Oxygen Delivery versus Oxygen Consumption

Philip E. James,*,[1] Melanie Madhani,*,† William Roebuck,‡ Simon K. Jackson,§ and Harold M. Swartz†

*Department of Cardiology and §Department of Medical Microbiology, Wales Heart Research Institute, University of Wales College of Medicine, Wales, United Kingdom; and †EPR Center, Radiology Department, and ‡Department of Pharmacology and Toxicology, Dartmouth Medical School, U.S.A.

Received May 1, 2001; published online August 17, 2001

***In vivo* EPR was used to investigate liver oxygenation in a hemodynamic model of septic shock in mice. Oxygen-sensitive material was introduced either (i) as a slurry of fine particles which localized at the liver sinusoids (pO_2 = 44.39 ± 5.13 mmHg) or (ii) as larger particles implanted directly into liver tissue to measure average pO_2 across the lobule (pO_2 = 4.56 ± 1.28 mmHg). Endotoxin caused decreases in pO_2 at both sites early (5–15 min) and at late time points (6 h after endotoxin; sinusoid = 11.22 ± 2.48 mmHg; lobule = 1.16 ± 0.42 mmHg). The overall pO_2 changes observed were similar (74.56% versus 74.72%, respectively). Blood pressures decreased transiently between 5 and 15 min (12.88 ± 8% decrease) and severely at 6 h (59 ± 9% decrease) following endotoxin, despite volume replacement with saline. Liver and circulatory nitric oxide was elevated at these times. Liver oxygen extraction decreased from 44% in controls to only 15% following endotoxin, despite severe liver hypoxia. Arterial oxygen saturation, blood flow (hepatic artery), and cardiac output were unaffected. Pretreatment with L-NMMA failed to improve endotoxin-induced oxygen defects at either site, whereas interleukin-13 preserved oxygenation. These site-specific measurements of pO_2 provide *in vivo* evidence that the principal cause of liver hypoxia during hypodynamic sepsis is reduced oxygen supply to the sinusoid and can be alleviated by maintaining sinusoidal perfusion.**

Key Words: **EPR; liver; hypoxia; sepsis.**

Endotoxin, a lipopolysaccharide (LPS) component of the Gram-negative bacterial cell wall induces sepsis in animal models and is the major cause of septic shock in patients (1). The latter is characterised by hypotension and altered tissue perfusion leading to multiple system organ failure (MSOF) (2). Although, the precise cause of organ dysfunction remains uncertain, much convincing evidence implicates nitric oxide (NO) overproduction leading to reduced oxygen supply and/or oxygen utilisation (3–5) in the pathogenesis of this condition.

The hepatic circulation, the portal blood supply, and sinusoidal perfusion are particularly affected. There is evidence that LPS-induced NO dilates blood vessels and causes hyperperfusion in some tissue areas and hypoperfusion in others (6, 7). Complete NOS inhibition with a non-specific inhibitor such as L-NMMA (affecting both cNOS and iNOS) alleviates LPS-induced hypotension, but causes enhanced sinusoid vasoconstriction, intravascular coagulation, and reduced perfusion. Therefore basal NO production appears to be essential for preventing disseminated intravascular coagulation (DIC) and maintenance of organ perfusion. Whether he-

[1] To whom correspondence and reprint requests should be addressed. Fax: (+44) 029 20 743739. E-mail: Jamespp@cf.ac.uk.

1089-8603/01 $35.00

patic NO is beneficial or harmful appears to depend upon the quantity of NO present (8, 9), which is in turn dependent on whether the time elapsed between the stimulus has been sufficient to elicit iNOS synthesis and thus excessive NO production (4, 10).

We have previously studied early effects of LPS *in vivo* (11). We undertook EPR (electron paramagnetic resonance) oximetry studies coupled with magnetic resonance imaging (MRI) and showed redistribution of oxygenated blood occurred in the kidney within minutes following LPS administration *in vivo*. We have also demonstrated how *in vivo* EPR can be utilized to simultaneously monitor liver pO_2 and NO during sepsis (12). We recently developed a technique that enabled measurement of pO_2 from specific anatomical sites within liver. To our knowledge, this allowed for the first time separate assessment of pO_2 at liver sinusoids and across the liver lobule during sepsis. We could therefore investigate how defective oxygen delivery and/or oxygen consumption contribute to altering liver pO_2. Physiological parameters were also measured in these animals (blood pressure, heart rate, and blood flow) so that circulatory effects could be distinguished from local changes in oxygenation. We took advantage of the fact that EPR could be used to make repeat *in vivo* measurements of pO_2 during septic shock.

MATERIALS AND METHODS

EPR Oximetry

In order to measure average pO_2 across the liver lobules or pO_2 selectively from liver sinusoids, gloxy (an oxygen-sensitive, paramagnetic material) was either injected directly into the liver as large particles or intravenously (i.v.) in the form of a suspension of fine microparticles, respectively. The spectral characteristics and oxygen-sensitivity of gloxy have been published previously (13). In brief, the EPR spectral linewidth obtained from gloxy is broadened by oxygen. The rate of change in linewidth is particularly sensitive at lower oxygen tensions (i.e., $<$30 mmHg) making it suitable for making measurements of pO_2 from tissue. The peak-to-peak linewidth was measured using a spectral simulation package (EWVoight software) and the pO_2 was calculated by calibrating against known oxygen tensions.

Measurement of pO_2 across the liver lobule. Typically, 2 days prior to the sepsis experiment, three 200-μm pieces of gloxy were injected through a 22 G needle. This needle was fitted with a length of wire so that the particles could be implanted at the desired location in the liver and report on pO_2. Particles were selected under a microscope using a haemocytometer for size reference.

Measurement of pO_2 from liver sinusoids. A suspension of fine particles of gloxy ("slurry") was prepared by manual grinding using a pestle and mortar, then sieving the gloxy through a mesh (20 μm). One hundred microliters of this suspension in pyrogen-free saline was injected directly into the lateral tail vein of mice. Using sequential sieving, we found the mean size of the gloxy in a typical slurry to be 2 μm, with 75% of material being <5 μm. We have used this technique previously with gloxy (13) and other materials (such as India Ink (14)) in order to deliver oxygen-sensitive material to liver sinusoids of animals.

We also undertook experiments in which gloxy slurry was injected directly into the liver. The rationale for these studies was to ensure that any differences in pO_2 observed could not be attributed to the fact that two different preparations of gloxy were used (such as might be expected if physical size of gloxy were an important parameter which might affect the spectral linewidth at a given pO_2).

Animals

All studies were approved by the Institutional Review Board for the care of animal subjects, and the care and handling of the animals were in accord with National Institutes of Health guidelines for ethical animal research. The experiments were performed on anaesthetised spontaneously breathing male Balb/C mice (approximately 22 g body weight). Isofluorane (1.4%) was introduced via a cone mask and inhalation gas consisted of air with oxygen added so that the final concentration of oxygen was 26%. Concentrations of anaesthesia and oxygen were monitored on-line using a Capnomac surgical gas analyzer. Core body temperature (measured rectally) was maintained at 37°C using a heated operating table. Mice were placed in a supine position between the EPR magnet poles so that the liver was

within the active volume of the detecting resonator and EPR spectra recorded repeatedly. Hemodynamic parameters were monitored via canulation of the left carotid artery with PE 10 tubing. This was linked via a small pressure transducer to an IBM driven Biopac system for recording of heart rate (HR) and mean arterial blood pressure (MABP). Sham-operated mice (without gloxy implantation) showed no differences in haemodynamic parameters that could be attributed to the implantation procedure.

EPR Measurement of NO and pO_2

A loop gap resonator ("whole body" resonator) 3.0 cm in diameter, with a 2-cm active region with two bridged gaps (designed and constructed in our laboratory) was used in conjunction with an EPR spectrometer equipped with a microwave bridge operating at 1.1 GHz. Over modulation of the spectral signal could lead to over estimation of spectral linewidth, and also affect signal amplitude. Spectrometer conditions were typically optimised either for recording of accurate linewidths from gloxy (a modulation amplitude approximately one third the observed linewidth was used as rule of thumb) or standard conditions in order to measure NO-Fe-$(DETC)_2$ signal amplitude.

In Vivo Measurement of Nitric Oxide (NO)

Mice were given (subcutaneously, lower leg muscle) ferrous sulfate (50 mg/kg) and disodium citrate dihydrate (250 mg/kg) in saline, followed by diethyldithiocarbamate (DETC) (250 mg/kg) was administered intraperitoneally (i.p.). Mice were then placed in a supine position between the EPR magnet poles so that the liver was within the active volume of the resonator. EPR spectra were recorded repeatedly (every 2 min) from 30 to 90 min post-DETC/Fe injection. In a typical experiment, we observed an increase in NO-Fe-$(DETC)_2$ signal after an initial delay of 20–30 min. This was followed by a plateau in signal amplitude (approximately 60 min after injection of DETC/Fe) reflecting an equilibrium being established between signal accumulation and signal clearance from the tissue. The maximum signal amplitude detected was used as a measure of $NO^{\bullet}$ level in each mouse. In order to measure the level of $NO^{\bullet}$ at a particular time point following injection of LPS, animals were injected with DETC/Fe at different times relative to the stimulus, allowing approximately 60 min for achieving peak EPR signal intensity. The advantages and limitations of this technique are discussed elsewhere, and we have previously utilized this technique to study tissue levels of NO in several animal model systems (13, 15). Recent literature also provides considerable controversy in regard to whether NOS produces NO or NO^- (nitroxyl anion) (16) and whether DETC (or its analogue, MGD) complexes with both these species (17). A complete discussion is beyond the scope of this manuscript, but we have found EPR detection of tissue NO-Fe-$(DETC)_2$ to agree closely with other measures of NO and activity of NOS both *in vitro* and *in vivo*.

Blood O_2

Blood samples were obtained using a cut-down procedure to gain access to either hepatic artery or vein. Blood (0.3 ml) was drawn into a 0.5-cc dry heparin-coated syringe and blood gases were assessed immediately on a standard clinical blood gas analyzer (Ciba-Corning 238). These studies were undertaken in separate groups of animals.

Septic Model and Experimental Protocol

Animals having had gloxy previously implanted in liver as slurry or particles were anaesthetised and equilibrated for 30 min prior to experimentation. Baseline pO_2 and haemodynamic measurements were made, then LPS (*E. coli* 0111:B4; Sigma; 1 mg/22 g body weight) was injected i.p. in 100 μl pyrogen-free saline. This model of LPS-induced septic shock is well established in our laboratory, typically peak NO levels are observed at 6 h and correspond with hypotension at this time. Control animals received the same volume of pyrogen-free saline only. Hemodynamic parameters and pO_2 were measured every 5 min until 30 min, then at 30-min intervals up to 6 h after LPS injection. Additional saline was administered (200 μl/30 min) via a carotid canula which also measured hemodynamic parameters.

N^G-monomethyl-L-arginine (LNMMA). LNMMA was administered i.p. (1 mg/22 g body weight) 30 min prior to LPS injection. NO and pO_2 measurements were carried out as above.

Interleukin-13 (IL-13). IL-13 was administered i.p at the same time as LPS (80 μg/22 g body weight). NO and pO_2 measurements were carried out as above.

Blood Flow

An ultrasound flow device (Transonic systems) was used to monitor blood flow through the hepatic artery. These measurements were relatively invasive and extremely sensitive to positioning of the flow probe (18), we therefore measured flow in separate groups of mice (i.e., flow was not measured in animals in which pO_2 and NO measurements were made). We ensured that implantation of gloxy itself (particles or slurry) had no effect on flow through the hepatic artery by comparing flow measurements in animals with and without prior gloxy implantation. Typically, in anesthetized animals an incision was made in the upper right peritoneal region. This was large enough to allow access to the hepatic vessels and placement of the flow probe. The shaft of the flow probe was 2 mm in diameter and semirigid, and was held in position using a micromanipulation device. The incision was closed and sutured around the probe shaft. Animals were then allowed to equilibrate for 30 min prior to taking flow readings. We had only limited success in our attempts to measure flow over a long time period (as in our 6 h sepsis model), we therefore focused our studies to taking flow readings every 5 min between 5.5 and 6.5 h post saline or LPS injection (in order to compare with pO_2 and $NO^{\cdot}$ measurements). In order to achieve this, surgery to position the flow probe was initiated 4 h into the septic episode.

Histology

The mice were sacrificed and the livers removed and embedded in paraffin. Five-micrometer slices were taken and lightly stained with hematoxilyn. We found that costaining with hematoxylin and eosin occasionally made it difficult to distinguish the gloxy (particles or slurry) from the darkly stained nuclear structures of the cells. Assessment of the anatomical positioning of the dark, black, particulate gloxy in liver (particles or slurry) was undertaken using light microscopy. One hundred random areas of interest were examined and Gloxy associated with either parenchymal (hepatocytes) or nonparenchymal (Kupffer or fibroblast) cells was assessed.

Ex Vivo Assays

Aspartate aminotransferase (AST). AST levels in serum were assessed using the Infinity Reagent Diagnostic Test (Sigma). Briefly, the reagent was placed into the cuvette and brought to 37°C. The serum sample was added directly to the cuvette (sample:reagent ratio was 1:10). Exactly 1 min after mixing, the absorbance (340 nm) was monitored every 30 s for 3 min.

Extent of lipid peroxidation (thiobarbituric acid reactive substances). TBARS, were measured in plasma using a previously described fluorometric technique (19). In brief, plasma or a standard solution of malondialdehyde (MDA) was added to thiobarbituric acid in acetic acid (29 mmol/l; pH 2.4) and heated for 1 h at 95°C. After the samples cooled, HCl (5 mol/L; pH 1.6) was added and the reaction mixture was extracted with *n*-butanol. The fluorescence of the butanol layer was measured at wavelengths of 525 nm for excitation and 547 nm for emission. The calibration curve was prepared with MDA standards of 0–0.5 nmol/tube. Coefficients of variation for within- and between-runs were 4 and 7%, respectively. Each sample was run in triplicate.

Measurement of NOS Protein Expression Using Western Blotting

Mice were treated for 6 h and sacrificed following anesthesia with isolflurane. Liver tissues were excised and were frozen in liquid nitrogen and stored at −80°C until tissue extraction.

Preparation of liver extracts. Frozen liver tissue was weighed and homogenized (Pierce Tissue Grinder kit) in boiling lysis buffer (10 mM Tris, pH 7.4, 1.0 mM sodium orthovanadate, 1.0% SDS). Protein was determined with a Micro Bovine Serum Albumin (BSA) Protein Assay Reagent kit (Pierce).

TABLE I

Liver NO, Oxygen Extraction, and Hemodynamic Data for Saline and LPS-Treated Mice

	0–15 min after treatment		360 min after treatment	
	Control	LPS	Control	LPS
MABP (Percentage decrease compared to −5 min)	3.06 ± 6.9	12.88 ± 8.7	2.15 ± 7.9	59.0 ± 9.4[a]
NO (arbitrary units)	89 ± 38	136 ± 40[a]	67 ± 27	805 ± 69[a]
AVD (%)	51 ± 6	49 ± 8	41 ± 5	15 ± 11[a]
Blood flow (ml/min)	6.4 ± 4.7	5.3 ± 3.9	5.6 ± 4.0	3.9 ± 5.7
Heart rate (beats per min)	333.0 ± 40.8	361.4 ± 53.4	346.3 ± 53.4	366.6 ± 30.4

[a] Indicates where values were significantly different from relevant controls ($P < 0.05$). MABP, mean arterial blood pressure; AVD, arteriovenous difference in oxygen content of blood; NO, hepatic level of nitric oxide measured by *in vivo* EPR.

NOS Western blot analysis. Tissue homogenates were heated for 5 min at 95°C in cracking buffer (1 ml 2-Mercaptoethanol, 2 ml Glycerol, 0.4 g SDS, 0.2 g PMSF (100×), 20 mg Bromophenol blue, 20 ml of Distilled water). The proteins (40 μg of protein (iNOS) or 20 μg of protein (eNOS)/lane) were then separated by SDS–polyacrylamide gel electrophoresis (PAGE) in 7.5% resolving gels and blotted onto nitrocellulose membranes (Hybond-ECL) in a semi-dry electrophoretic transfer cell (Trans-Blot, Bio-Rad). Nitrocellulose membranes were incubated in blocking solution (4.5 g NaCl; 0.6 g Tris; 250 μl Tween 20 made up to 500 ml with distilled water) overnight at room temperature. The membranes were incubated for two hours at room temperature with either mouse monoclonal anti-iNOS (Transduction Laboratories) diluted 1:2500 in blocking solution or rabbit polyclonal anti-eNOS (Transduction Laboratories) diluted 1:1000 in blocking solution. Thereafter, membranes were washed five times for 30 min in washing solution (4.5 g NaCl; 250 μl Tween 20 made up to 500 ml with distilled water). They were then incubated for 2 h at room temperature with the secondary antibody (rabbit anti-mouse HRP conjugate (Sigma) for iNOS or goat anti-rabbit HRP conjugate (Sigma) for eNOS) diluted 1:10,000 in blocking buffer. The membranes were then washed five times for 30 min in washing buffer and developed using ECL plus detection kit (Amersham) according to the protocol supplied by Amersham. Finally, the chemiluminescence signal were detected with photographic film (Hyperfilm ECL; Amersham Pharmacia Biotech) and recorded after 5 to 10 min exposure.

Statistics

Results are expressed as the mean ± SD of n animals. Statistical evaluation unless otherwise stated was performed by one-way analysis of variance (ANOVA) followed by the Newman–Keuls test for multiple comparison, $^{**}P < 0.001$ and $^{*}P < 0.01$. Statistical analysis was undertaken using Prism software.

RESULTS

Effect of LPS Injection on Nitric Oxide and Hemodynamic Parameters

EPR detectable levels of NO-Fe-$(DETC)_2$ remained similar to baseline values in saline treated controls but increased significantly 6 h following LPS (67 ± 27 au versus 583 ± 270 au, respectively) (Table I). NO-Fe-$(DETC)_2$ levels were essentially the same in mice with gloxy particles compared to gloxy slurry (particle = 644 ± 78 au, slurry = 533 ± 147 au). We also measured a large increase in NO metabolites in plasma (nitrite and nitrate (NOx) according to the method of Misko *et al.* (20)) at 6 h (Control = 75.22 ± 34.41 μM; LPS = 444.37 ± 83.89 μM; $n = 6$ each). No significant increase in NOx was observed 15 min after LPS injection (data not shown).

Levels of iNOS measured at 6 h in liver tissue were markedly increased in LPS-treated animals compared to saline treated controls (density analysis of iNOS bands was 1.43 ± 0.70 versus 0.54 ± 0.48, respectively; $P < 0.05$; $n = 5$). Low levels of eNOS

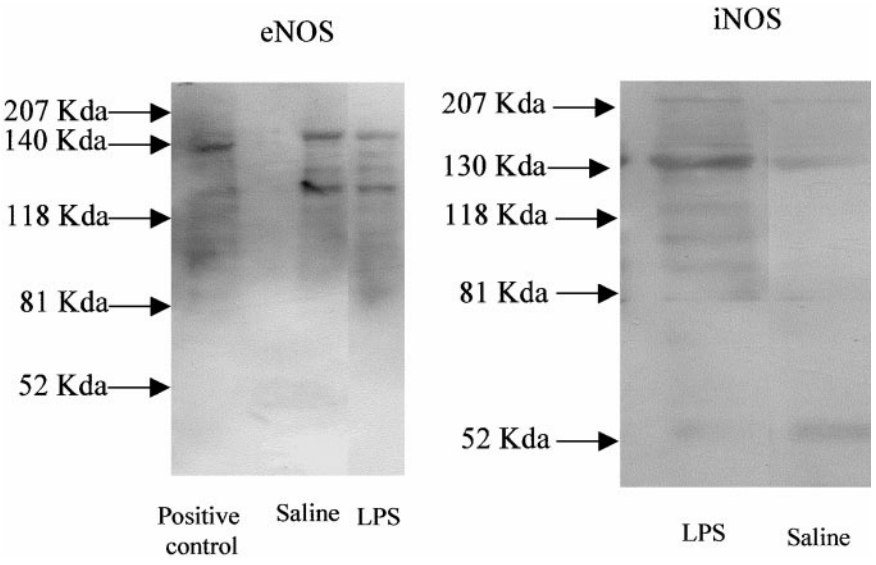

FIG. 1. Western blot analysis of protein extracts from liver tissue of mice subjected to saline or LPS treatment. Extracts were probed for (a) eNOS (140 kDa) or (b) iNOS (130 kDa).

were detected in both groups, but no upregulation by LPS (Fig. 1).

Mean arterial blood pressure (MABP) remained stable throughout the investigation period in control animals. LPS treatment resulted in a characteristic fall in MABP; a 13% decrease was observed within 15 min before returning to baseline. Minimum values occurred at 6 h (59%) (Table I).

Typically this bolus LPS model of sepsis, we found no evidence of enhanced lipid peroxidation (TBARS in plasma; control = 4.99 ± 0.84 versus LPS = 7.11 ± 3.96 nmol/ml, respectively; $P = 0.31$) or liver dysfunction (plasma AST; control = 380.8 ± 214.6 versus LPS = 621.5 ± 141.5 U/l; $P = 0.11$) as a result of LPS treatment.

Effect of LPS on Liver Oxygenation

Liver pO_2 measured from each site (sinusoid versus average lobule pO_2) after treatment with LPS or saline are summarized in Fig. 2. Early (0–15 min) and late time points (6 h) are shown, because tissue pO_2, NO, and circulatory hemodynamics returned to baseline values at intermediate times. We have also previously shown these times corresponded with stimulated production of NO (12).

In control animals, liver pO_2 varied according to the anatomical site from which pO_2 measurements were made (average lobule pO_2 was 4.56 ± 1.28 mmHg, whereas that from sinusoids was 44.39 ± 5.13 mmHg). Slurry injected directly into liver tissue showed pO_2 values that were between those found for the same material injected i.v. and by direct particle implantation (direct slurry pO_2 = 23.65 ± 8.45 mmHg). Although *in vitro* calibration showed gloxy particles had slightly different linewidth sensitivity to oxygen when compared to a slurry of the same material, tests using both materials at the same oxygen tensions resulted in the same pO_2 when recalculated from the appropriate calibration curves. We also found that slurry injected directly into liver tissue distributed over a broad tissue area. This resulted in pO_2 being sampled across a region that was several fold larger than that sampled by direct implantation of particles and not from a specific anatomical location (as with i.v. slurry localizing in sinusoids).

Endotoxin caused decreases in pO_2 at early and late time points and the overall pO_2 change observed at each tissue site was similar (74.56 versus 74.72% for liver lobule and sinusoid, respectively). The difference in pO_2 measured between sinusoid and lobule reflected oxygen utilisation across this region of tissue. This oxygen difference decreased from 39.8 mmHg in control animals to 10.0 mmHg after LPS (reflecting a decrease of 74.8%).

The arteriovenous difference in oxygen content

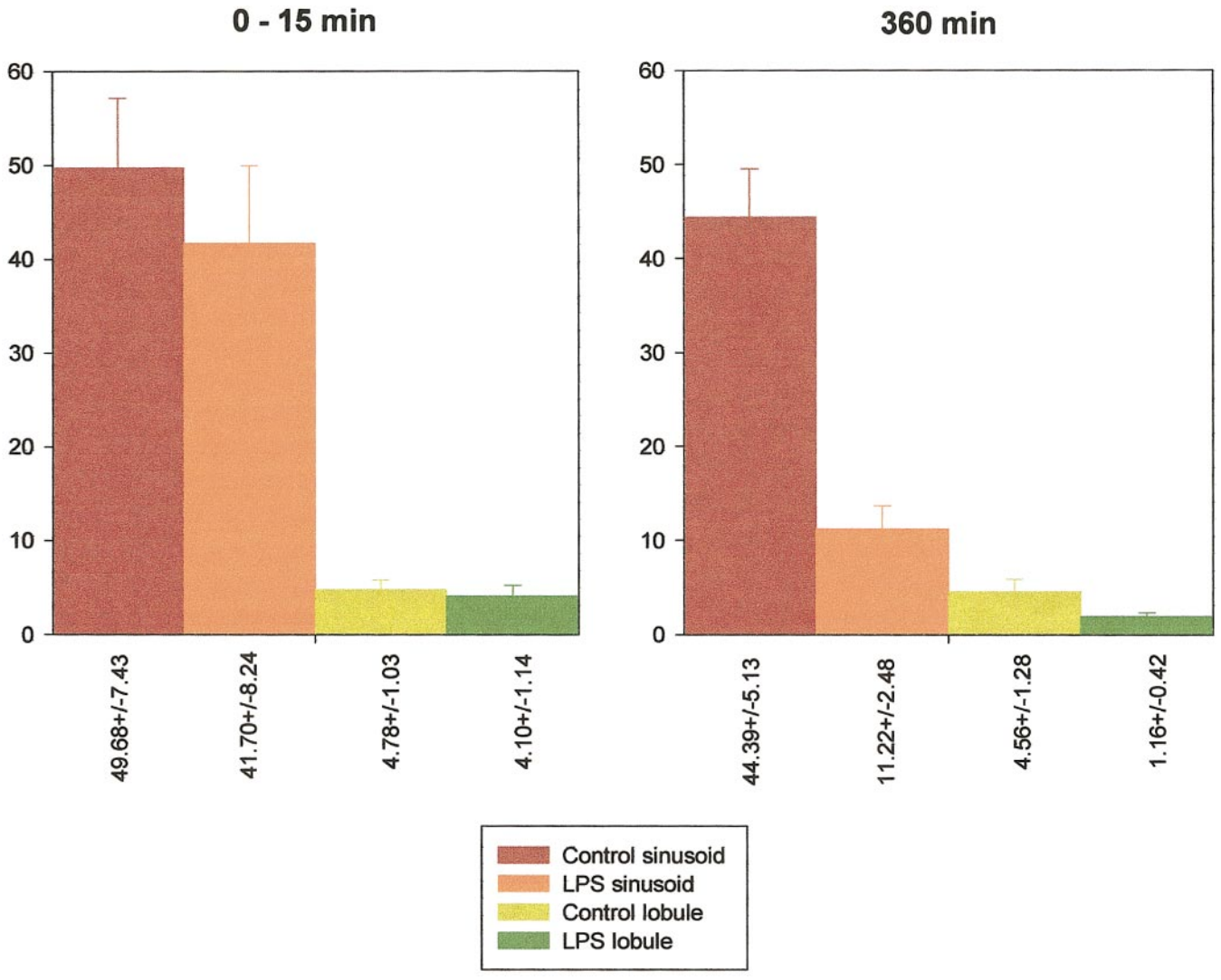

FIG. 2. Summarizes pO_2 data at early (<15 min) and late (360 min) time points after LPS.

(AVD) of blood, measured from hepatic artery and hepatic vein, respectively, was 51% in control animals at the beginning of the experiment (0–15 min). This was essentially the same in LPS-treated animals at this time (49%) despite the significant decrease in MABP. The AVD remained relatively high in control animals even at 6 h, whereas AVD decreased continuously in the LPS-treated group (reduced to 15% at 6 h). Arterial oxygen saturation remained >85% in both control and septic animals. Blood flow through the hepatic artery at 6 h was essentially the same in control versus LPS-treated animals. However, we acknowledge the high degree of variability within the treatment groups and between individual mice. This factor may have made measurement of smaller differences in blood flow difficult to detect. These data are also summarized in Table I.

Localization of Oxygen-Sensitive Material in Liver

Histological assessment of liver tissue slices revealed important findings central to the hypothesis being proposed in this paper. Although preparation and slicing of the tissue block caused disruption and usually removal of the large gloxy particles, a large

TABLE II

Summary of pO_2 Data 360 Min Posttreatment

pO_2 (mmHg)	Slurry	Particle	Slurry-particle pO_2 difference
Control	44.4 ± 5.1	4.6 ± 1.3	39.8
LPS	11.2 ± 2.5	1.2 ± 0.4	10.0
L-NMMA	14.7 ± 3.2	3.6 ± 0.8	11.1
IL-13	34.8 ± 6.4	4.9 ± 2.0	29.9

number of gloxy particles (or fragments of the larger particle) remained and filled a well described lesion. Surrounding this small elliptical lesion and interfacing with apparently normal hepatic tissue was a layer a few to several cells thick. There was no definitive evidence that the gloxy particle or fragments of it were distributed from the site of implantation. The site of particle implantation appeared to be at random and generally covered an area of tissue that included all hepatic tissue regions across the sinusoids and hepatic parenchyma. The linewidths obtained from implanted gloxy particles therefore reflected average pO_2 across the hepatic lobule. Examination of gloxy slurry in liver slices was difficult. However, in order to determine where in the liver the gloxy resided, we examined the location of gloxy slurry in 100 sites of interest. We found 13% of the slurry localised within the sinusoidal spaces. The remainder was mainly distributed either with intimate contact with hepatocytes (50%) or nonparenchymal cells (31%), such as fibroblasts or Kupffer cells. In no case was evidence found of incorporation of these particles into cells of any phenotype. Also, we found no evidence of a reaction of the particle with the tissue in which it was lodged or retained.

Inhibition of Nitric Oxide Production

In separate groups of animals, either L-NMMA (to abolish NO derived from both cNOS and iNOS (5, 9, 21)) or IL-13 (preventing iNOS expression (22)) treatment was administered 30 min prior to LPS injection. NO and pO_2 measurements were carried out as for control and LPS only animals. The pO_2 data are summarized in Table II. The pO_2 difference following LPS and L-NMMA treatment was similar to that observed in animals given LPS alone. IL-13 treatment alleviated hypoxia at both sites, and resulted in a pO_2 difference of 29 mmHg (reflecting a decrease of 27.4% compared to controls). MABP was characteristically increased following L-NMMA to controls and also to mice given LPS (118 and 108% at 6 h, respectively). IL-13 treatment caused a decrease in MABP (11% decrease compared to controls) that was not as severe as LPS alone (59% decrease). Circulating NO-metabolites (NOx) were reduced to control values (L-NMMA = 93.9 ± 39.4 and IL-13 = 103.9 ± 41 μM; n = 6 each), whereas NO-Fe-$(DETC)_2$ in liver was decreased 80 and 65%, respectively (L-NMMA = 161.0 ± 47.1 and IL-13 = 281.8 ± 52.0 arbitrary EPR units with spectrometer conditions normalized to control values).

DISCUSSION

Novel EPR methodology was used to make *in vivo* measurements of hepatic pO_2 and NO in a mouse model of sepsis. pO_2 was measured both across the liver lobule and selectively from hepatic sinusoids, enabling separate assessment of oxygen supply to and oxygen consumption across the liver lobule. Decreases in tissue oxygenation were observed at early and late time points and were closely associated with characteristic decreases in blood pressure and elevated NO. Our studies pretreating mice with L-NMMA showed no improvement in LPS-induced liver hypoxia despite alleviating systemic hypotension. IL-13 treatment alleviated both LPS-induced liver hypoxia and hypotension.

MABP decreased transiently 0–15 min following LPS injection (12.88 ± 8%), although this decrease was not as severe compared with 6 h (59 ± 9% decrease). The latter coincided with overproduction of NO (measured both as NOx in blood samples and liver NO-Fe-$(DETC)_2$). Liver iNOS expression was also upregulated at this time, whereas eNOS was essentially similar in control and LPS animals.

The hepatic circulation comprises a dual blood supply, whose arterial and portal venous components converge in the liver sinusoids and have a common outlet via the hepatic vein (23). Hepatic arterial flow accounts for only 25% of the total blood supply to the liver, but supplies most of the oxygen. Hepatic blood flow was unaltered in our studies, and taken together with normal cardiac output, it is

tempting to speculate that flow should not be considered an invariable criterion of the LPS-induced pO_2 changes seen in our studies. Similar findings have been found in clinical studies of septic shock (24). However, Pastor *et al.* (25) demonstrated a 25% decrease in hepatic arterial flow in rabbits following LPS administration. We must acknowledge therefore our results cannot completely rule out the possibility of transient or small overall effects of LPS on hepatic arterial flow, given the limits of sensitivity and practical difficulties associated with making accurate measurements of vascular blood flow in mice.

Early patient studies identified sepsis as primarily a low-flow perfusion system based on ineffective volume or cardiac failure (26). More recently, it has also been hypothesized that with adequate fluid therapy, tissue perfusion may be corrected early, thereby relieving the end-results of prolonged shock (27). In our studies, a subgroup of animals treated with LPS also received saline i.v. periodically throughout the investigation period. We did not expand the study to investigate volume replacement with plasma or other colloid, but cardiac output was similar to controls in these animals, suggesting fluid resuscitation was sufficient. We found volume replacement with saline was ineffective in alleviating the LPS-induced effects on liver oxygenation and inadequate perfusion.

A bolus LPS injection to animals provides a sepsis model in which to study circulatory and local hemodynamic changes. Oxidative damage to liver occurs only at later time points (10–11 h) following this dose of LPS, as demonstrated by MacMicking and colleagues (6). We found no evidence of lipid peroxidation or liver dysfunction up to 6 h following LPS injection. Alternative sepsis models involve priming animals with galactosamine followed by a much lower LPS dose, or injection of live bacteria, which reduces the LD_{50} for LPS. This induces enhanced liver damage (5), but the extent and timing of oxidative damage and liver dysfunction also varies considerably (7, 28), and generally give rise to an elevated host response.

In our studies, liver pO_2 varied according to the anatomical site from which pO_2 measurements were made. The fine gloxy slurry injected i.v. resided primarily within the sinusoids themselves and with Kupffer or fibroblast cells lining the sinusoidal lumen. These were in intimate contact with highly oxygenated blood (44.39 $\pm$ 5.13 mmHg), whereas the larger particles measured average pO_2 across the lobule (4.56 $\pm$ 1.28 mmHg), including sinusoids, nonparenchymal cells, and areas of packed parenchymal cells actively consuming the supplied oxygen.

Within liver, blood flows from the periphery to the centre of the lobule. Consequently, oxygen and metabolites, as well as other toxic or nontoxic substances, reach first the peripheral cells and then the central cells of the lobule. There is also a change from oxidative to nonoxidative metabolism (29). Our studies show a pO_2 gradient exists between the sinusoidal lumen and surrounding cells, and is largely dependent on cellular oxygen consumption (reflected by a comparatively low pO_2 reported from gloxy particles implanted in the lobule). This agrees closely with previous studies demonstrating anatomical variation in hepatic pO_2 (14, 30).

LPS treatment resulted in a 75% decrease in pO_2 measured at both anatomical sites. This is particularly important because if delivery of oxygenated blood to the sinusoid would have remained the same as in control animals, the pO_2 reported from the sinusoids would not have changed significantly. It is plausible that decreased sinusoid pO_2 following LPS could be explained in terms of increased oxygen consumption by cells close to the sinusoid (such as Kupffer cells) and this might also have given rise to a pO_2 decrease across the lobule. We therefore measured hepatic artery and venous blood pO_2 and oxygen saturation. Arterial oxygen saturation was $>$85% even in LPS-treated animals. Liver oxygen extraction decreased from 41% in control animals to 15% following LPS. Thus, venous blood had unusually high oxygen content, despite tissue hypoxia, and it is unlikely that our findings could be explained in terms of localized increases in oxygen consumption close to the sinusoid.

The narrowed AVD across the liver may be explained in terms of either LPS-induced impairment of overall liver oxygen consumption or the presence of arteriovenous shunts bypassing the sinusoid capillary beds. Our site-selective measurements of pO_2 provide strong evidence that 6 h following LPS treatment, blood supply (and hence oxygen) to the sinusoids was impaired by approximately 75%,

rather than LPS-induced inhibition of oxygen consumption across the lobule.

The pO_2 difference between sinusoid and lobule (slurry pO_2-particle pO_2) was considered an indirect measure of oxygen utilization between these sites. In control livers, this pO_2 difference was 39.83 mmHg, whereas following LPS, this decreased to 10.05 mmHg. This was probably the result of cells in the mid- to inner region of the lobule operating under almost ischemic conditions (lobule pO_2 was 1.16 ± 0.42 mmHg 6 h following LPS) rather than inhibited mitochondrial consumption per se. Other responses to the hypoxic conditions experienced deep in the lobule parenchyma may also have activated transcription of genes whose protein products facilitated metabolic adaptation to hypoxia (31).

LPS also caused early decreases in pO_2 at both slurry and particle sites (within 15 min) accompanied by changes in NO and MABP. We have previously shown LPS-induced early changes in pO_2 accompanied by redistribution of blood in the kidney *in vivo* (11). These effects were also NO mediated. Although the early changes observed in the present study were not as severe as those observed 6 h, it is likely these early events participate in initiating the cascade of lethal events, which have severe pathophysiological consequences later during a septic episode.

Our studies pre-treating mice with L-NMMA or IL-13 produced several additional key findings. First, complete inhibition of NOS by L-NMMA did not alleviate LPS-induced effects on oxygen supply, oxygen consumption, and liver pO_2. This agrees with data obtained by other groups in similar models in which L-NMMA treatment augmented LPS-induced liver damage (5, 25). This further supports the view that maintenance of a critical level of NO is essential to providing sufficient sinusoidal perfusion. Second, IL-13 is known to inhibit NO production by iNOS (22). IL-13 forms part of the cascade of anti-inflammatory mediators in response to infection (31). Our data would suggest IL-13 effectively alleviated LPS-induced changes in pO_2, possibly by maintaining only adequate levels of NO to preserve sinusoidal perfusion without systemic hypotension. IL-13 also improved oxygen utilization across the lobule.

CONCLUSIONS

In summary, we show that LPS induces liver hypoxia late (6 h) during sepsis and is likely to be the result of reduced oxygen delivery. This coincides with overproduction of NO and reduced overall oxygen extraction across the liver. Our selective measurements of pO_2 *in vivo* implicate decreased blood supply to the sinusoids as the major contributing factor, rather than NO-induced inhibition of cellular oxygen utilization. Non-selective inhibition of NO biosynthesis was ineffective in preventing these pO_2 changes, whereas IL-13 treatment (to inhibit iNOS) alleviated the hypoxic condition. The techniques employed here provide a new way to assess LPS-induced defects in oxygen supply versus oxygen consumption *in vivo*.

ACKNOWLEDGMENTS

This study was supported by NIH Grant PO1 GM51630 and used the facilities of the EPR Center for Viable Biological Studies, supported by NIH Grant P41 RR11602. The Department of Cardiology, Wales Heart Research Institute, is supported by the British Heart Foundation. The authors also thank Denise Mac Millan and Stalina Grinberg for their excellent technical assistance.

REFERENCES

1. Cobb, J. P., and Danner, R. L. (1996). Nitric oxide and septic shock. *J. Am. Med. Assoc.* **275,** 1192–1196.
2. Wright, C. E., Rees, D. D., and Moncada, S. (1992). Protective and pathological roles of nitric oxide in endotoxic shock. *Cardiovasc. Res.* **26,** 48–57.
3. Sair, M., Etherington, P. J., Curzen, N. P., Winlove, C. P., and Evans, T. (1996). Tissue oxygenation and perfusion in endotoxemia. *Am. J. Physiol.* **271,** H1620–H1625.
4. Vos, T. A., Gouw, A. S. H., Kloc, P. A., *et al.* (1997). Differential effects of nitric oxide synthase inhibitors on endotoxin-induced liver damage in rats. *Gastroenterology* **113,** 1323–1333.
5. Di Silvio, M., Nussler, A. K., Geller, D. A., and Billiar, T. R. (1996). A role for nitric oxide in liver inflammation and infection. *In* Nitric Oxide: Principles and Actions (Lancaster, J. Jr., Ed.), pp. 219–236, Academic Press.
6. Mac Micking, J. D., Nathan, C., Hom, G., Chartrain, N., Fletcher, D. S., Trumbauer, M., Stevens, K., Xie, Q.-W., Sokoi, K., Hutchinson, N., Chen, H., and Mudgett, J. S. (1995). Altered responses to bacterial infection and endotoxic shock in mice lacking inducible nitric oxide synthase. *Cell* **81,** 641–650.

7. Teale, D. M., and Atkinson, A. M. (1992). Inhibition of nitric oxide synthesis improves survival in murine peritonitis model of sepsis that is not cured by antibiotics alone. *J. Antimic. Chemo.* **30,** 839–842.
8. Nathan, C. F., and Stuehr, D. J. (1990). Does endothelium-derived nitric oxide have a role in cytokine-induced hypotension? *J. Natl. Cancer Inst.* **82,** 726–728.
9. Nathan, C., and Xie, Q.-W. (1994). Nitric oxide synthases: Roles, tolls, controls. *Cell* **78,** 915–918.
10. Szabo, C., Aalzman, A. L., and Ischiropoulos, H. (1995). Endotoxin triggers the expression of an inducible isoform of nitric oxide synthase and the formation of peroxynitrite in the rat aorta *in vivo*. *FEBS Lett.* **363,** 235–238.
11. James, P. E., Bacic, G., Grinberg, O., Goda, F., Jackson, S. K., Dunn, J., and Swartz, H. M. (1995). Renal oxygenation during endotoxemia as monitored by *in vivo* EPR oximetry and MR imaging. *Free Rad. Biol. Med.* **21,** 25–34.
12. James, P. E., Miyake, M., and Swartz, H. M. (1999). Simultaneous measurement of NO and pO_2 from tissue by in vivo EPR. *Nitric Oxide Chem. Biol.* **3**(4), 292–301.
13. James, P. E., Grinberg, O. Y., Goda, F., O'Hara, J. A., and Swartz, H. M. (1997). Gloxy: An oxygen-sensitive coal for accurate measurement of low oxygen tensions in biological systems. *Magn. Res. Med.* **38,** 48–58.
14. Jiang, J., Nakashima, T., Liu, K. J., Goda, F., Shima, T., and Swartz, H. M. (1996). Measurement of pO_2 in liver using EPR oximetry. *J. Appl. Physiol.* **80**(2), 552–558.
15. Berliner, L. J., Khramtsov, V., Fujii, H., and Clanton, T. L. (2001). Unique *in vivo* applications of spin traps. *Free Rad. Biol. Med.* **30,** 489–499.
16. Xia, Y., and Zweier, J. L. (1997). Direct measurement of nitric oxide generation from nitric oxide synthase. *Proc. Natl. Acad. Sci. USA* **94,** 12705–12710.
17. Xia, Y., Cardounel, A. J., Vanin, A. F., and Zweier, J. L. (2000). Electron paramagnetic resonance spectroscopy with *N*-methyl-D-glucamine dithiocarbamate iron complexes distinguishes nitric oxide and nitroxyl anion in a redox-dependent manner: Applications in identifying nitrogen monoxide products from nitric oxide synthase. *Free Rad. Biol. Med.* **29,** 793–797.
18. D'Almeida, M. S., Gaudin, C., and Lubrec, D. (1995). Validation of 1- and 2-mm transit-time ultrasound flow probes on mesenteric artery and aorta of rats. *Am. J. Physiol.* **268,** H1368–H1372.
19. Wasowicz, W., Neve, J., and Peretz, A. (1993). Optimized steps in fluorometric determination of thiobarbituric acid reactive substances in serum: Importance of extraction pH and influence of sample preservation and storage. *Clin. Chem.* **39,** 2522–2526.
20. Misko, T. P., Schilling, R. J., Salvemini, D., Moore, W. M., and Currie, M. G. (1993). A fluorometric assay for the measurement of nitrite in biological samples. *Anal. Biochem.* **214,** 11–16.
21. Harbrecht, B. G., and Billiar, T. R. (1995). The role of nitric oxide in Kupffer cell-hepatocyte interactions. *Shock* **3,** 79–877.
22. Berkman, N., Robichaud, A., Robbins, R. A., Roesems, G., Haddad, E. B., Barnes, P. J., and Chung, K. F. (1996). Inhibition of iNOS expression by IL-4 and IL-13 in human lung epithelial cells. *Immunology* **89,** 363–367.
23. Blumgart, L. H. (Ed.) (1994). *In* Surgery of the Liver and Billiary Tract, 2nd ed., p. 97, Churchill Livingsone, Edinburgh.
24. Mc Lean, A. P. H., Duff, J. H., Groves, A. C., Lapointe, R., and Mac Lean, L. D. (1971). Oxygen uptake in septic shock. *In* Septic Shock in Man (Hershey, S. G., Del Guercio, L. R. M., and McConn, R., Eds.), pp. 107–115, Little, Brown, Boston.
25. Pastor, C. M., and Payen, D. M. (1994). Effect of modifying nitric oxide pathway on liver circulation in a rabbit endotoxin shock model. *Shock* **2,** 196–202.
26. Siegel, J. H., Greenspan, M., and Del Guercio, L. R. M. (1967). Abnormal vascular tone, defective oxygen transport and myocardial failure in human septic shock. *Ann. Surg.* **165,** 504–517.
27. Mori, E., Hasebe, M., Kobayashi, K., and Iijima, N. (1987). Alterations in metabolite levels in carbohydrate and nergy metabolism of rat in haemorrhagic shock and sepsis. *Metabolism* **36,** 14–20.
28. Jacobson, D., and Singer, M. (1996). The cell, the mitochondrion, oxygen and sepsis. *Int. Care Emergency Med.* 263–274.
29. Moore, K. L., and Dalley, A. F. (Eds.) (1999). Clinically oriented anatomy. *In* Anatomy, 4th ed., Chap. 2, pp. 175–331, Lippincott, Williams and Wilkins, London.
30. Nakashima, T., Jiang, J., Goda, F., Shima, T., and Swartz, H. M. (1995). The measurement of pO_2 in mouse liver *in vivo* by EPR oximetry using india ink. *Magn. Reson. Med.* **6,** 158–160.
31. Semenza, G. L. (2000). Expression of hypoxia-inducible factor 1: Mechanisms and consequences. *Biochem. Pharmacol.* **59,** 47–53.